Sakarya Üniversitesi Fen Bilimleri Dergisi
Sakarya University Journal of Science
e-ISSN : 2147-835X
Publisher : Sakarya University
Vol. 29, No. 6, 717-725, 2025
DOI: https://doi.org/10.16984/saufenbilder.1755797
Research Article

An Egret Swarm Optimization Based BiRNN Method Approach to Determine the Protective Stopping Time of UR3 Robot Arm

Göksu Taş[1*], Cafer Bal[2]

[1] Department of Mechatronics Engineering, Manisa Celal Bayar University, Manisa, Türkiye, goksu.tas@cbu.edu.tr, ror.org/053f2w588
[2] Department of Mechatronics Engineering, Technology Faculty, Fırat University, Elazig, Türkiye, cbal@firat.edu.tr, ror.org/05teb7b63
[*]Corresponding Author

ARTICLE INFO

Keywords:
UR3 Robot arm
Egret swarm optimization
Bidirectional recurrent neural Network
Emergency stop

Article History:
Received: 06.08.2025
Revised: 21.10.2025
Accepted: 17.11.2025
Online Available: 14.12.2025

ABSTRACT

The emergency stop moment is of critical importance for robots to meet legal and industrial safety requirements, protect human health and equipment, and respond quickly in times of crisis. In this study, the emergency stop time of the UR3 robot arm, which is widely used in the industry, was determined according to the axis speed, current value, and temperature values. The emergency stop moment of the robot was determined successfully with the state-of-the-art deep learning models. The performance of the state-of-the-art deep learning models was compared using the most common classification metrics. In addition, the most important hyperparameter values of the Bidirectional Recurrent Neural Network method were determined using the Egret Swarm Optimization Algorithm, which is new in literature. Among all models, the ESOA-BiRNN model was the most successful method with a value of 0.946124 according to the ROC AUC metric. The success of the proposed method is given together with other classification metrics.

1. Introduction

The term "human-robot collaboration" (HRC) describes how humans and robots cooperate to accomplish tasks in a shared workspace [1]. The fourth industrial revolution's technical advancements have an impact on the current dynamic and fiercely competitive global market [2]. Manufacturing firms that want to improve their market position by switching from mass production to mass customisation are very interested in collaborative robots. To fulfill the ever-increasing demands for flexibility, efficiency, product variations, and time-to-market, this paradigm shift necessitates the adoption of sophisticated and sustainable production systems, which are distinguished by a scalable degree of industrial automation. In this regard, collaborative robots makes it possible to combine the advantages of industrial automation with the indispensable cognitive human qualities, therefore enhancing the performance of production systems and the welfare of workers [3]. Therefore, COllaborative RoBOTs (i.e., cobots) may do repetitive and difficult tasks, either cognitively or physically, while relieving human operators. Cobots have been used in a variety of fields outside of industry, including agriculture, education, and medicine [4, 5].

Benefits on production cost, performance, and sustainability are usually highlighted in the business case for robots and other industrial automation [6]. There are two schools of thought about advanced automation and robotics from the perspective of worker safety. Though recent analyses using Census of Fatal Occupational Injuries (CFOI) data indicate a low rate of fatal injuries with robots between 1992 and 2017, these technologies have been linked to certain catastrophic injuries. On the other hand, the positive health/safety perspective acknowledges the advantages of removing human workers from performing the so-called "dirty, dull, and

Cite as: G. Taş, C. Bal, “An Egret Swarm Optimization Based BiRNN Method Approach to Determine the Protective Stopping Time of UR3 Robot Arm,” Sakarya University Journal of Science, vol. 29, no. 6, pp. 717-725, 2025. https://doi.org/10.16984/saufenbilder.1755797

dangerous" tasks [7] as well as the ways in which robotic technologies can reduce exposures and physical demands on human workers [8]. Although just one new technology deployment was implemented with the primary goal of worker well-being, a 2001 Department of Energy (DOE) study of 68 new technology deployments at DOE sites revealed that 71% had a moderate to high potential of lowering occupational exposures [9]. Positive effects on workplace safety and health are frequently cited as a (wanted) byproduct of new technologies.

Even while collaborative modes have become safer generally over time, it is still crucial to develop and deploy ergonomic and intrinsically safe automation systems so that people may work alongside robots without fear of injury. Furthermore, human unpredictability and the complexity of automation systems in use push for new approaches to risk assessment and hazard analysis in collaborative settings. Naturally, in order to guarantee the most seamless and effective manufacturing processes, safety restrictions must advance at the same rate as collaborative systems' performance needs [10]. Therefore, this study aims to improve the safety of human-robot interactions by conducting a deep learning-based study. Recent studies on robot operational safety and machine learning-based studies have been reviewed in the literature. Fuzzy inference and sensor fusion methods are used by [11] to regulate robot velocity while maintaining system productivity and safety. The sensor fusion technique uses a machine learning approach to process images obtained from several depth sensors as well as those from a thermal camera.

According to [12], present methods for measuring the distance between humans and robots are challenging and inaccurate. In order to create a control framework based on DT that enables the quick and precise measurement of the minimum safe distance between humans and robots, the authors concentrate on the pre-collision stage. Consequently, several safety robot tactics are used to prevent collisions. Future research must, however, enhance data processing and transmission capabilities, and abrupt and moving obstructions in the surrounding environment must be appropriately controlled as possible crash causes.

In accordance with ISO TS 15066's SSM approach, Zanchettin and Lacevic [13] offer a real-time technique for guiding a robotic manipulator along a designated path while maximizing safety and productivity (i.e., minimal time of completion). A mathematical programming model for the best planning and distribution of disassembly duties among the worker, robot, and HRC is developed and solved by Lee et al. [14]. Subject to safety and resource limitations, the goal is to reduce the overall disassembly time. Regarding the safety restrictions, a minimum safety distance is necessary to prevent potential accidents and human injuries during disassembly. The Modified Extended State Observer (MESO) method and the robot dynamic model are combined by Ren et al. [15] to identify collisions quickly and reliably. They also provide information on the direction and amplitude of force signals resulting from a broad class of actuator defects. It has been found in the literature that many problems have been solved with deep learning studies. [16, 17].

A review of the literature reveals that many studies have been conducted to ensure safe and reliable human-robot interactions, utilizing machine learning or artificial intelligence. In this study, the stopping moment of the UR3 robot manipulator was successfully determined using a deep learning-based metaheuristic optimization. This study uses a unique metaheuristic optimization strategy to optimize the deep learning model's main hyperparameters and give more accurate and dependable prediction performance.

Developing an optimization-supported deep learning method (ESOA-BiRNN) to ascertain a UR3 robot arm's protective stopping time is the aim of this research. The study's premise is that, in comparison to conventional deep learning models and other optimization techniques, combining Egret Swarm Optimization with BiRNN enhances predictive accuracy.

2. Matherial and Methods

This study used a dataset taken from another study [18]. The software was developed using the Python programming language. Optimization studies were conducted on a personal computer running the Ubuntu operating system.

2.1. UR3 robot

The UR3e is one of the smallest industrial collaborative robot arms. Its small size provides great advantages when automating activities in confined spaces, such as on benchtops or inside production equipment. Table 1 shows the specifications of the UR3e robot arm [19].

Table 1. UR3e robot arm specifications

Parameter	Value
Reach	500 mm/19.7 in
Payload	3 kg/ 6.6 ıbs
Footprint	128 mm
Weight	11.2 kg

The UR3e is ideal for a collaborative and industrial robot due to its small size. The UR3e is designed to increase efficiency in limited workspaces and offers unparalleled precision and flexibility. The cobot can be integrated into a table for human workers or as a separate workstation to perform tasks such as picking, assembling and placing parts. With its small footprint and lightweight design, the UR3e seamlessly integrates into any production environment, complementing human workers and increasing productivity. This collaborative robot includes state-of-the-art safety features to ensure safe collaboration between humans and machines [19]. Figure 1 shows the UR3 robot and some of the equipment required to stop a robot.

This study's dataset (UR3 CobotOps dataset: [18]) was sourced from the UCI Machine Learning Repository, which is openly accessible. The 7410 samples in the dataset are divided into 7077 non-stopping events and 278 protective halting events. Multiple sensor readings are included in each sample, including cycle information, protective stop signals, grip status, joint currents (J0–J5), joint temperatures (T0–T5), and joint speeds (J0–J5). The dataset was split 80:20 between training and testing sets at random for the purpose of developing the model. The test set was only used to assess performance; the training set was utilized to learn the model.

2.2. Egret swarm optimization algorithm

Zuyan Chen et al. introduced the Egret Swarm Optimization Algorithm in 2022. The three primary components of snowy and great egret predatory behavior sit-and-wait strategy, aggressive strategy, and discriminant conditions are the inspiration for ESOA. Groups of egret teams, each consisting of three egrets, can make up an egret population. In the aggressive strategy, Egrets A, B, and C, respectively, use the random walk and encirclement mechanism, whereas

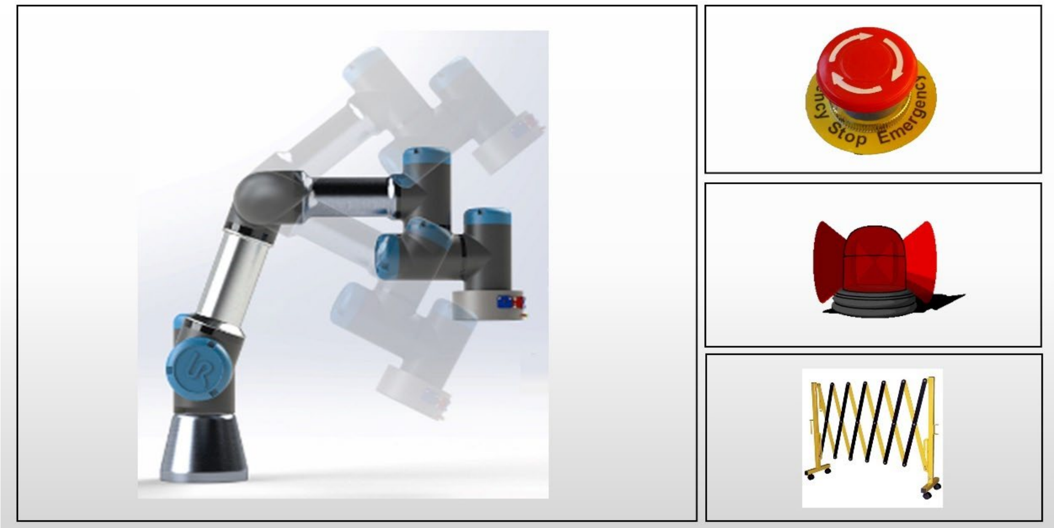

Figure 1. UR3 stopping moment

Egret A uses the sit-and-wait approach [20]. An egret swarm flock is shown in Figure 2.

Figure 2. Egret swarm

While egrets who use an aggressive approach will actively seek prey, those that use a sit-and-wait approach will wait silently for a meal to come. Regarding energy usage and revenue generation, these two approaches differ from one another. The sit-and-wait approach uses little energy, but its earnings are comparatively steady. Nevertheless, the aggressive approach uses more energy, but it might yield greater rewards.

Motivated by these two approaches, the ESOA views potential solutions as distinct individuals inside the egret swarm and mimics the egret swarm's predation behavior to choose the best solution. The three primary components of the algorithm are the discriminative condition, aggressive strategy, and sit-and-wait strategy. Three egrets are found in each of the n egret squads that make up each egret colony. Of them, Egret A uses the sit-and-wait tactic, whilst Egrets B and C use the aggressive strategy's random walk and bounding mechanism, respectively. Egret A updates its location using the observation equation, Egret B utilizes a random walk, and Egret C employs a boundary technique.
The position of each egret is updated according to its fitness, which is determined independently for each iteration. In particular, it is updated if the new fitness value is higher; if not, it is updated with a specific probability [21]. The three components of ESOA—the Discriminant Condition, the Aggressive Strategy, and the Sit-And Wait Strategy—are explained in more depth below. Guiding Forward is the Sit-And-Wait Strategy used by Snowy Egret A. Here, the Observation Equation is constructed to model the Snowy Egret's estimation technique of the potential presence of prey in its current position. One way to parameterize the Observation Equation is as [22]

$$\hat{y}_i = w_i \cdot x_i \tag{1}$$

where y_i is the estimated value of prey at the current location; ω_i is the weight of the observation equation; and x_i is the position of the *i-th* egret squad. To assess the prediction's accuracy, the error e_i is specified here and can be computed by

$$e_i = \|\hat{y}_i - y_i\|^2/2 \tag{2}$$

where y_i denotes the prey's actual value in its present location. Using the gradient descent approach and the errors determined in the equation above, the weights in the observation equation are adjusted. After defining the gradient di of the weights, the direction di prediction is finally finished using the gradient.

$$\hat{g}_i = \frac{\partial e_i}{\partial \omega_i} = (\hat{y}_i - y_i) \cdot x_i \tag{3}$$

$$\hat{d}_i = \hat{g}_i / |\hat{g}_i|$$

ESOA defines $d_{h,i}$ and $d_{g,i}$ to better characterize egret learning behavior. The $d_{h,i}$ indicates the direction change based on the same group of egrets' optimal location. The direction change done in accordance with each egret's ideal position is shown by $d_{g,i}$ [23].

$$d_{h,i} = \frac{x_{ibest} - x_i}{|x_{ibest} - x_i|} \cdot \frac{f_{ibest} - f_i}{|x_{ibest} - x_i|} + d_{ibest} \tag{4}$$

$$d_{g,i} = \frac{x_{gbest} - x_i}{|x_{gbest} - x_i|} \cdot \frac{f_{gbest} - f_i}{|x_{gbest} - x_i|} + d_{gbest} \tag{5}$$

When the global historical ideal position is represented by x_{gbest} and the individual historical optimal position by x_{ibest}. The objective function is denoted by *f*. Based on the same group of egrets' ideal position, dibest indicates the historical optimal direction change. The historical optimal direction change based on the allegrets' ideal position is indicated by the symbol dgbest. It is possible to obtain the integrated gradient $\hat{g}_i$ equation using (3-5).

$$\hat{g}_i = (1 - r_h - r_g) \cdot d_i + r_h \cdot d_{b,i} + r_g \cdot d_{g,i} \tag{6}$$

where the random numbers r_h and r_g range from 0 to 0.5. The Snowy Egret's position is updated

where r_{bi} is a random number in (−π/2, π/2) and $x_{b,i}$ is Snowy Egret B's most recent position. The aggressive strategy employed by Egret C is represented by an encircling mechanism, and its position $x_{c,i}$ update formula is as follows [23]

$$x_{c,i} = (1 - r_b - r_g)x_i + r_b(x_{ibest} - x_i) + r_g(x_{gbest} - x_i) \tag{12}$$

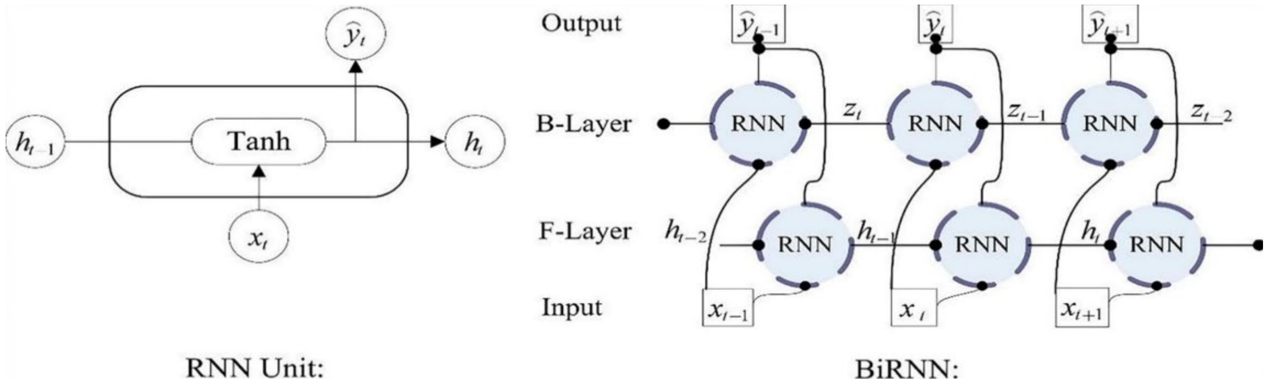

Figure 3. BiRNN architecture [25]

using the integrated gradient determined by the equation above.

$$x_{a,i} = x_i + \exp(-t/(0.1 \cdot t_{max})) \cdot 0.1 \cdot hop \cdot g_i \tag{7}$$

where t is the current number of iterations, t_{max} is the total number of iterations, and *hop* is the egret colony's search range, or the difference between the higher and lower limits of the independent variable. $x_{a,i}$ represents the Snowy Egret A's updated position. Lastly, the following equation [23] is used to update the weights of the observation equations.

$$m'_i = \beta_1 \cdot v_i + (1 - \beta_2) \cdot g_i \tag{8}$$

$$v'_i = \beta_2 \cdot v_i + (1 - \beta_2) \cdot g_i \odot g_i \tag{9}$$

$$w'_i = w_i - m_i/\sqrt{v_i} \tag{10}$$

where β_1 is 0.9 and β_2 is 0.99, and m and v are intermediate variables for updating w. The following equation [23] describes the predatory behavior of Egret B, which employs an aggressive strategy that manifests as random search:

$$x_{b,i} = x_i + tan\,(r_{b,i}) \cdot bop/(1 + t) \tag{11}$$

Each egret's position inside a group of egrets is about to be identified, according to Equation 7. Because each group of egrets must behave in unison under ESOA, the group's final destination is decided by discriminant conditions. First, the values of the fitness functions corresponding to $x_{a,i}$, $x_{b,i}$, and $x_{c,i}$ are calculated, and the least one is chosen as the outcome of this iteration. This is how the discriminant condition principle is explained. The outcome is kept if it is better than the previous iteration's outcome or if the random generation number (r) is less than 0.3. One way to characterize the procedure is [23, 22]

$$f(x) = |f(x_{a,i})f(x_{b,i})f(x_{c,i})| \tag{13}$$

$$c_i = argmin(f(x)) \tag{14}$$

2.3. Bidirectional recurrent neural network

Forward RNN and backward RNN make up the BiRNN as a presented Figure 3. The BiRNN carries out further reverse feature processing based on the forward feature processing of the sequence data. The bidirectional correlation between sensors may be completely taken into account by this character. The forward operation was completed by the first unit of the robot data input sequence data x^j_{i-1} entering the first RNN cell, and the reverse operation was completed by the final unit of the robot data input sequence data x_{i-4}^{j} entering the second RNN cell. Ultimately, the output hidden layer sequence $h_{i1}^{j}, h_{i2}^{j}, h_{i3}^{j}, h_{i4}^{j}$ was obtained by concatenating the output results of the forward and reverse calculations [24].

$$z_t = f(x_t \bar{w}_{xz} + z_{t+1}\bar{w}_{zz} + d_z) \tag{15}$$

$$h_t = f(x_t \bar{w}_{xh} + h_{t-1}\bar{w}_{hh} + d_h) \tag{16}$$

$$y_t = U\left(h_t \bar{w}_{hy} + z_t \bar{w}_{zy} + d_y\right) \tag{17}$$

where h_t and z_t are the stored information in the forward layer (F-Layer) and backward layer (B-Layer), *f()* and *U()* are the activation functions, x_t and y_t are the input and output characteristics of the t_{th} sample, and h_t 1 displays the stored information of the *t-1th* sample in the F-Layer and z_{t+1} displays the stored information of the $t+1_{th}$ sample in the B-Layer. The deviation vectors of the forward hidden layer, the backward hidden layer, and the output layer are denoted by d_h, d_z, and d_y, respectively. The weight coefficients between the input and hidden layers are denoted by $\bar{w}_{xh}$ and $\bar{w}_{xz}$, the weight coefficients between the hidden layers by $\bar{w}_{hh}$ and $\bar{w}_{zz}$, and the weight coefficients between the output and hidden layers by $\bar{w}_{hy}$ and $\bar{w}_{zy}$ [25].

3. Results

The optimization algorithm used the -accuracy metric while using the fitness function in the search space. By selecting min from the minmax value, the accuracy value was essentially tried to be maximized. Table 2 shows the parameter values of ESOA. The number of agents used in this study is given with the pop_size metric. With the iteration parameter, deep learning training is done with 10 epochs, while training is performed at each iteration, and appropriate values are obtained from the search space with five iterations.

Table 2. Parameter values of the optimization algorithm

Parameter	Value
Iteration	5
Population size	5

Table 3 shows the fitness values obtained for the -accuracy fitness function in this study. Due to parameters such as dataset size, size of deep learning models, and number of iterations, the parameters of the deep learning model were obtained with two separate searches with the optimization algorithm.

Table 3. Fitness values achieved by the optimization algorithm

Parameter	Fitness
Learning rate & units	0.9639700651168823
Beta_1 & batch size	0.9619306325912476

Table 4 shows the results obtained for this problem using the most commonly used performance metrics in classification problems with artificial intelligence. According to the ROC AUC metric, which indicates the general discrimination power, the ESOA-BiRNN method achieved the most successful discrimination power with a value of 0.946124. The confusion matrix resulting from the classification is given in Figure 4. The result of the most successful method, the ESOA-BiRNN model, is shown. It predicted 1254 no moments correctly, while 149 no moments were predicted as yes. While 58 peak values correctly predicted the stopping moment, 10 moments were predicted incorrectly. By optimizing BiRNN's hyperparameters (learning rate, hidden units, etc.), ESOA improves generalization and lessens overfitting.

In Table 5, the parameters that most affect the performance of the deep learning algorithm, namely learning rate, batch size, units, and beta_1, were determined by ESOA in this study. In the second column of the table, the optimization algorithm gives the search area of the hyperparameters. During the search area, the algorithm tries to find the most appropriate value by trial and error. The hyperparameter values found by the optimization are given in the third column.

In order to predict stopping points more precisely, BiRNN simultaneously learns past and future dependencies in time-series data. Hyperparameter optimization studies have not been thoroughly investigated because the ESOA optimization approach is relatively new in the literature.

Table 4. Prediction results of deep learning models

Model	F1-Score	Recall	Accuracy	Precision	ROC AUC
CNN	0.219731	0.720588	0.763426	0.12963	0.802073
LSTM	0.190909	0.617647	0.757988	0.112903	0.736625
BiLSTM	0.219718	0.573529	0.811693	0.135889	0.782734
GRU	0.144254	0.867647	0.524133	0.078667	0.817146
BiRNN	0.396104	0.897059	0.873555	0.254167	0.940946
CNN-RNN	0.225053	0.779412	0.751869	0.131514	0.854283
ESOA-BiRNN	0.421818	0.852941	0.89191	0.280193	**0.946124**
TCN	0.259136	0.573529	0.848402	0.167382	0.764916

Table 5. Metaheuristic optimization algorithm search result

Parameter	Area	Found
Learning rate	0.000001-0.01	0.000464879172
Batch size	16-128	17
Units	16-512	127
Beta_1	0.8-0.9999	0.95906069

As a result, our work offers one of the earliest uses of ESOA for deep learning model hyperparameter adjustment, showcasing its potential to improve prediction robustness and accuracy in robot safety applications.

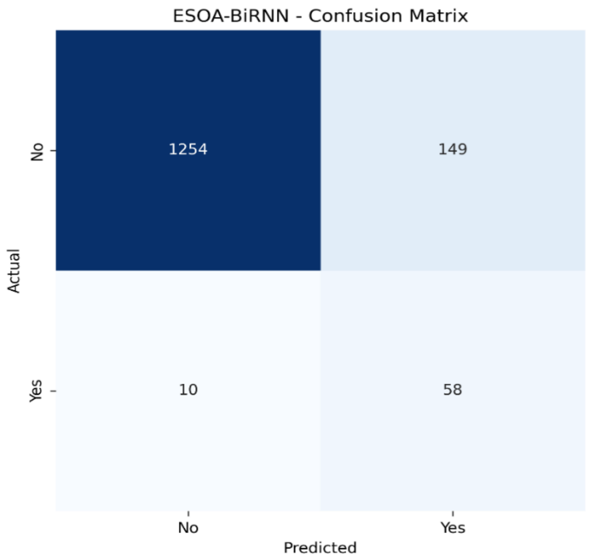

Figure 4. Confusion matrix resulting from the training of the ESOA-BiRNN model

4. Conclusion

In this study, an optimization-assisted deep learning model was developed to ensure the safe operation of industrial robot manipulators. Successfully determining the stopping moment of robot manipulators using deep learning methods is crucial for reasons such as ensuring human safety, protecting equipment and production, and adhering to legal standards. Robot-human interaction has recently become increasingly sensitive due to safety and production issues. The safe and reliable operation of robots in industry is crucial. Therefore, in this study, the stopping moment of the UR3 robot arm was successfully predicted using an optimization-assisted deep learning algorithm.

Furthermore, the most important hyperparameter values of the BiRNN method were successfully determined using the ESOA metaheuristic algorithm, a new method in the literature. The proposed model achieved 94.61% success in inter-class prediction. Furthermore, a total of eight deep learning models were compared, and the ESAO-BiRNN method was found to be the most successful. The authors plan to work on identifying connection problems between different robot types in the industry in future studies.

In conclusion, this study presented ESOA-BiRNN, an optimization-supported deep learning technique, to forecast the UR3 robot arm's protective stopping time. In contrast to traditional models, this work's primary contribution is the incorporation of a novel optimization method (ESOA) with BiRNN to improve hyperparameter tuning, which led to increased predictive accuracy. The results have significant industrial ramifications in addition to their scholarly value. For safe human–robot cooperation in production settings, accurate protective stopping time calculation is essential, and our suggested approach offers a workable solution that can be incorporated into industrial safety systems. Future research should concentrate on testing using real-time experimental settings, expanding the approach to various collaborative robot models, and investigating more hybrid optimization–deep learning combinations.

Article Information Form

Acknowledgments

The UR3 CobotOps dataset used in this study was provided via the UCI Machine Learning Repository, for which t he authors are grateful. It can be found at: https://archive.ics.uci.edu/dataset/963/ur3+cobotops.

Authors' Contribution

G.T: Methodology, Research, Experimental Study, Data editing, Manuscript writing and editing, C.B: Research, Manuscript writing and editing. All authors have read and agreed to the published version of the manuscript.

The Declaration of Conflict of Interest/ Common Interest

No conflict of interest or common interest has been declared by authors.

Artificial Intelligence Statement

No artificial intelligence tools were used while writing this article.

References

[1] M. Rüßmann, M. Lorenz, P. Gerbert, M. Waldner, J. Justus, P. Engel, et al., "Industry 4.0: The future of productivity and growth in manufacturing industries," Boston consulting group, vol. 9, no. 1, pp. 54–89, 2015.

[2] A. Jamwal, R. Agrawal, M. Sharma, and A. Giallanza, "Industry 4.0 Technologies for manufacturing sustainability: A systematic review and future research directions," Applied Sciences, vol. 11, no. 12, Art. no. 12, Jan. 2021.

[3] B. Siciliano, O. Khatib, Eds., Springer Handbook of Robotics. Berlin, Heidelberg: Springer Berlin Heidelberg, 2008.

[4] V. Moysiadis, D. Katikaridis, L. Benos, P. Busato, A. Anagnostis, D. Kateris, et al., "An integrated real-time hand gesture recognition framework for human–robot interaction in agriculture," Applied Sciences, vol. 12, no. 16, Art. no. 16, Jan. 2022.

[5] A. Amarillo, E. Sanchez, J. Caceres, and J. Oñativia, "Collaborative human–robot interaction interface: Development for a spinal surgery robotic assistant," Int J of Soc Robotics, vol. 13, no. 6, pp. 1473–1484, Sep. 2021.

[6] J. Ogbemhe, K. Mpofu, N. S. Tlale, "Achieving sustainability in manufacturing using robotic methodologies," Procedia Manufacturing, vol. 8, pp. 440–446, Jan. 2017.

[7] L. Takayama, W. Ju, C. Nass, "Beyond dirty, dangerous and dull: What everyday people think robots should do," in Proceedings of the 3rd ACM/IEEE international conference on Human robot interaction, in HRI '08. New York, NY, USA: Association for Computing Machinery, Mar. 2008, pp. 25–32.

[8] C. Thomas, L. Stankiewicz, A. Grötsch, S. Wischniewski, J. Deuse, and B. Kuhlenkötter, "Intuitive work assistance by reciprocal human-robot interaction in the subject area of direct human-robot collaboration," Procedia CIRP, vol. 44, pp. 275–280, Jan. 2016.

[9] D. Oakley, "Science and technology contributions to ımproving worker safety and health", Accessed: Jul. 28, 2025. [Online]. Available: https://archivedproceedings.econference.io/wmsym/2001/29/29-2.pdf

[10] L. Gualtieri, E. Rauch, and R. Vidoni, "Emerging research fields in safety and ergonomics in industrial collaborative robotics: A systematic literature review," Robotics and Computer-Integrated Manufacturing, vol. 67, p. 101998, Feb. 2021.

[11] M. Costanzo, G. De Maria, G. Lettera, and C. Natale, “A multimodal approach to human safety in collaborative robotic workcells,” IEEE Transactions on Automation Science and Engineering, vol. 19, no. 2, pp. 1202–1216, Apr. 2022.

[12] H. Li, W. Ma, H. Wang, G. Liu, X. Wen, Y. Zhang, et al., “A framework and method for Human-Robot cooperative safe control based on digital twin,” Advanced Engineering Informatics, vol. 53, p. 101701, Aug. 2022.

[13] A. M. Zanchettin and B. Lacevic, “Safe and minimum-time path-following problem for collaborative industrial robots,” Journal of Manufacturing Systems, vol. 65, pp. 686–693, Oct. 2022.

[14] M.-L. Lee, S. Behdad, X. Liang, M. Zheng, “Task allocation and planning for product disassembly with human–robot collaboration,” Robotics and Computer-Integrated Manufacturing, vol. 76, p. 102306, Aug. 2022.

[15] T. Ren, Y. Dong, D. Wu, K. Chen, “Collision detection and identification for robot manipulators based on extended state observer,” Control Engineering Practice, vol. 79, pp. 144–153, Oct. 2018.

[16] G. S. Karabay, M. Çavaş, E. Avcı, “Çiçek Sınıflandırmada AlexNet ve MobileNetV2 mimarilerinin performans karşılaştırması,” GUMMFD, vol. 40, no. 2, Feb. 2025.

[17] K. Usanmaz, S. Güney, “Derin öğrenme yöntemleriyle trafik işaretlerinin gerçek zamanlı sınıflandırılması,” GUMMFD, vol. 40, no. 2, Feb. 2025.

[18] M. Tyrovolas, K. Aliev, D. Antonelli, C. Stylios, “UR3 CobotOps,” UCI Machine Learning Repository, 2024.

[19] “UR3e Ultra-lightweight, compact cobot.” Accessed: May 05, 2025. [Online]. Available: https://www.universal-robots.com/products/ur3e/

[20] T. Li, Y. Liu, Z. Chen, “Application of sine cosine egret swarm optimization algorithm in gas turbine cooling system,” Systems, vol. 10, no. 6, Dec. 2022.

[21] P. Wei, M. Shang, J. Zhou, X. Shi, “Efficient adaptive learning rate for convolutional neural network based on quadratic interpolation egret swarm optimization algorithm,” Heliyon, vol. 10, no. 18, Sep. 2024.

[22] Y. Liu, C. Yu, D. Li, L. Wang, X. Li, H. Li, F. Wang, “An optimization capacity design method of household integrated energy system based on multi-objective egret swarm optimization,” IET Renewable Power Generation, vol. 17, no. 8, pp. 1993–2008, 2023.

[23] Z. Chen, A. Francis, S. Li, B. Liao, D. Xiao, T. T. Ha, et al., “Egret swarm optimization algorithm: An evolutionary computation approach for model free optimization,” Biomimetics, vol. 7, no. 4, Dec. 2022.

[24] Z. Wang, Y. Lii, X. He, R. Yan, Z. Li, Y. Jiang, et al., “Improved deep bidirectional recurrent neural network for learning the cross-sensitivity rules of gas sensor array,” Sensors and Actuators B: Chemical, vol. 401, p. 134996, Feb. 2024.

[25] W. Zhou, D. Luo, “The hesitant fuzzy BiRNN based on twice-cycle mechanism and its intelligent applications,” Expert Systems with Applications, vol. 237, p. 121655, Mar. 2024.